

Preferential interaction coefficient for nucleic acids and other cylindrical poly-ions

Emmanuel Trizac*

CNRS; Univ. Paris Sud, UMR8626, LPTMS, ORSAY CEDEX, F-91405 and
Center for Theoretical Biological Physics, UC San Diego,
9500 Gilman Drive MC 0374 - La Jolla, CA 92093-0374, USA

Gabriel Téllez†

Departamento de Física, Universidad de Los Andes, Apartado Aéreo 4976, Bogotá, Colombia

The thermodynamics of nucleic acid processes is heavily affected by the electric double-layer of micro-ions around the polyions. We focus here on the Coulombic contribution to the salt-polyelectrolyte preferential interaction (Donnan) coefficient and we report extremely accurate analytical expressions valid in the range of low salt concentration (when polyion radius is smaller than the Debye length). The analysis is performed at Poisson-Boltzmann level, in cylindrical geometry, with emphasis on highly charged poly-ions (beyond “counter-ion condensation”). The results hold for any electrolyte of the form $z_-:z_+$. We also obtain a remarkably accurate expression for the electric potential in the vicinity of the poly-ion.

Coulombic interactions between salt and poly-anions play a key role in the equilibrium and kinetics of nucleic acid processes [1]. A convenient quantity quantifying such interactions and allowing for the analysis and interpretation of their thermodynamics consequences, is the so called preferential interaction coefficient. Several definitions have been proposed and their interrelation studied, see e.g. [2, 3, 4]. In the present work, they are defined as the integrated deficit (with respect to bulk conditions) of co-ions concentration around a rod-like poly-ion. Our goal is to provide analytical expressions describing the effect of salt concentration and poly-ion structural parameters on the preferential interaction coefficient, for a broad class of asymmetric electrolytes. For symmetric electrolytes, it will be shown that our formulas improve upon existing analytical results. For other asymmetries, they seem to have no counterpart in the literature. Our analysis holds for highly (i.e. beyond counter-ion condensation [5, 6]) and uniformly charged cylindrical poly-ions, and is explicitly limited to the low salt regime (i.e. when the poly-ion radius a is smaller than the Debye length $1/\kappa$). These conditions are most relevant for RNA or DNA in their single, double, or triple strand forms.

As in several previous approaches [7, 8, 9, 10], we adopt the mean-field framework of Poisson-Boltzmann equation, in a homogeneous dielectric background of permittivity ϵ . The same starting point has proven relevant for related structural physical chemistry studies of nucleic acids [11]. In a $z_-:z_+$ electrolyte, the dimensionless electrostatic potential $\phi = e\varphi/kT$ (with $e > 0$ the elementary charge and kT thermal energy) then obeys the equation [12]

$$\frac{1}{r} \frac{d}{dr} \left(r \frac{d\phi}{dr} \right) = \frac{\kappa^2}{z_+ + z_-} [e^{z_-\phi} - e^{-z_+\phi}], \quad (1)$$

where r is the radial distance to the rod axis. The valencies z_+ and z_- of salt ions are both taken positive. Denoting derivative with a prime, the boundary conditions read $r\phi'(r) = 2\xi > 0$ at the polyion radius ($r = a$) and $\phi \rightarrow 0$ for $r \rightarrow \infty$. The latter condition expresses the infinite dilution of poly-ion limit and ensures that the whole system is electrically neutral, since it (indirectly) implies that $r\phi' \rightarrow 0$ for $r \rightarrow \infty$. We consider a negatively charged poly-anion for which $\phi < 0$ and the line charge density reads $\lambda = -e\xi/\ell_B < 0$, where $\ell_B = e^2/(\epsilon kT)$ denotes the Bjerrum length (0.71 nm in water at room temperature). Finally, the Debye length is defined from the bulk ionic densities n_+^∞ and n_-^∞ through $\kappa^2 = 4\pi\ell_B(z_+^2 n_+^\infty + z_-^2 n_-^\infty)$.

The Coulombic contribution to the anionic preferential interaction coefficient is defined as [7, 8, 9, 10, 13]

$$\Gamma = \kappa^2 \int_a^\infty (e^{z_-\phi} - 1) r dr, \quad (2)$$

while its cationic counterpart follows from electro-neutrality. This quantity –which provides a measure of the Donnan effect [14]– can be expressed in closed form as a function of the electrostatic potential, see Appendix A. As can be seen in (A3) and (A4), Γ depends exponentially on the surface potential ϕ_0 , so that deriving a precise analytical expression is a challenging task. Furthermore, we are interested here in the limit $\kappa a < 1$ (including the regime $\kappa a \ll 1$) which is analytically more difficult than the opposite high salt situation where to leading order, the charged rod behaves as an infinite plane, and curvature corrections can be perturbatively included [15, 16, 17].

We will proceed in two steps. Focusing first on the surface potential $\phi_0 = \phi(a)$, we make use of recent results [18] that have been obtained from a mapping of Eq. (1) onto a Painlevé type III problem [19, 20, 21]. The exact expressions thereby derived only hold for 1:1, 1:2 and 2:1 electrolytes, but may be written in a way that is electrolyte independent. This remarkable feature is spe-

*Electronic address: trizac@lptms.u-psud.fr

†Electronic address: gtellez@uniandes.edu.co

z_+/z_-	1/10	1/3	1/2	1	2	3	10
\mathcal{C}	-2.51	-1.94	-1.763	-1.502	-1.301	-1.21	-1.06

TABLE I: Values of \mathcal{C} appearing in Eq. (4) as a function of electrolyte asymmetries. For $z_+/z_- = 1, 1/2$ and 2 , \mathcal{C} is known analytically from the results of [18]. The corresponding values are recalled in Appendix B. For other values of z_+/z_- , \mathcal{C} has been determined numerically, see in particular Fig. 6 of Appendix B.

cific to the short distance behaviour of ϕ and has been overlooked so far, since not only short distance but also large distance properties have been studied [18]. We are then led to conjecture that the corresponding expression holds for *any* binary electrolyte $z_-:z_+$, and we explicitly check the relevance of our assumption on several specific examples.

Technical details are deferred to the appendices. It is in particular concluded in Appendix B that the surface potential may be written

$$e^{-z_+\phi_0} \simeq \frac{2(z_+ + z_-)}{z_+(\kappa a)^2} [(z_+\xi - 1)^2 + \tilde{\mu}^2] \quad (3)$$

where

$$\tilde{\mu} \simeq \frac{-\pi}{\log(\kappa a) + \mathcal{C} - (z_+\xi - 1)^{-1}}. \quad (4)$$

Expression (4) is valid for $\kappa a < 1$ and $z_+\xi > 1$ [in fact $z_+\xi > 1 + \mathcal{O}(1/|\log \kappa a|)$]. These conditions are easily fulfilled for nucleic acids. The ‘‘constant’’ \mathcal{C} appearing in (3) depends smoothly on the ratio z_+/z_- but is otherwise salt and charge independent. We report in Table I its values for several electrolyte asymmetries. The decrease (in absolute value) of \mathcal{C} when z_+/z_- increases is a signature of more efficient (non-linear) screening with counter-ions of higher valencies.

From Eq. (3) and the results of Appendix B, our approximation for Γ takes a simple form

$$\Gamma \simeq -\frac{z_-}{z_+} (1 + \tilde{\mu}^2). \quad (5)$$

This expression is tested in Figures 1 and 2 against the ‘‘true’’ numerical results that serve as a benchmark. In Fig. 1 which corresponds to a monovalent salt (or more generally a $z:z$ electrolyte), we also show the prediction of Ref. [9], which is, to our knowledge, the most accurate existing formula for a 1:1 salt. For the technical reasons discussed in Appendix B, and that are evidenced in Figure 6, our expression improves that of Shkel, Tsodikov and Record [9], particularly at lower salt content. For 1:2 and 2:1 salts, we expect Eq. (5) to be also accurate, since it is based on exact expansions. The situation of other salt asymmetries is more conjectural (see Appendix B), but Eq. (5) is nevertheless in remarkable agreement

with the full solution of Eq. (1), see Fig. 2. To be specific, in both Figures 1 and 2, the relative accuracy of our approximation is better than 0.2% for $\kappa a = 10^{-2}$ (for both ss and ds RNA parameters). At $\kappa a = 0.1$, the accuracy is on the order of 1%.

As illustrated in Fig. 3, approximation (4) assumes that $z_+\xi > 1$. The corresponding expression for Γ therefore breaks down when ξ is too low. More general expressions, still for $\kappa a < 1$, may be found in appendix C. The inset of Fig. 3 offers an illustration and shows that the limitations of approximation (4) may be circumvented at little cost, providing a quasi-exact value for Γ . Moreover, it is shown in this appendix that for $z_+\xi = 1$, $\tilde{\mu}$ reads

$$\tilde{\mu} \simeq \frac{-\pi/2}{\log(\kappa a) + \mathcal{C}}. \quad (6)$$

On the other hand, Eq. (3) still holds. The corresponding Γ is shown in Fig. 4.

We provide in Appendix C a general expression of the short scale (i.e valid up to $\kappa r \sim 1$) radial dependence of the electric potential, see Eq. (C1). The bare charge should not be too low [more precisely, one must have $\xi > \xi_c$ with ξ_c given by Eq. (C5)], and $\tilde{\mu}$ —which encodes the dependence on ξ^- follows from solving Eq. (C2). In general, the corresponding solution should be found numerically. However, one can show *a)* that $\tilde{\mu}$ vanishes for $\xi = \xi_c$, *b)* that $\tilde{\mu}$ takes the value (6) when $z_+\xi = 1$ and *c)* that $\tilde{\mu}$ is given by (4) when $z_+\xi$ exceeds unity by a small and salt dependent amount. In practice, for DNA and RNA, we have $\xi > 2$ and Eq. (4) provides

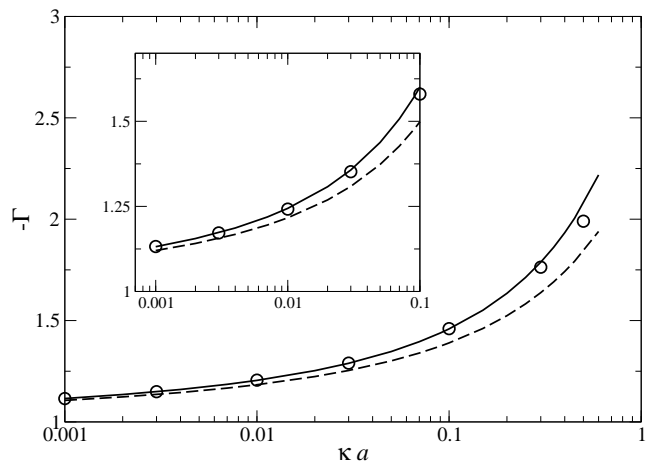


FIG. 1: Preferential interaction coefficient for a 1:1 salt. The main graph corresponds to ss-RNA with reduced line charge $\xi = 2.2$ while the inset is for ds-RNA ($\xi = 5$). The circles correspond to the value of (2) following from the numerical solution of Eq. (1). The prediction of Eq. (5) with $\tilde{\mu}$ given by (4) and $\mathcal{C} \simeq -1.502$, shown with the continuous curve, is compared to that of Ref. [9], shown with the dashed line. As in all other figures, the opposite of Γ is displayed, to consider a positive quantity.

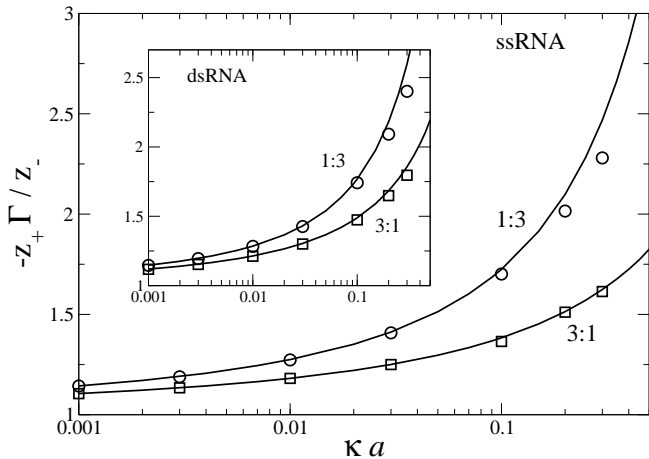


FIG. 2: Same as Figure 1 for a 1:3 and a 3:1 electrolyte. From Table I, we have $\mathcal{C} \simeq -1.21$ in the 1:3 case and conversely $\mathcal{C} \simeq -1.94$ in the 3:1 case. The symbols correspond to the numerical solution of Eq. (1) and the continuous curves show the results of Eq. (5) with again $\tilde{\mu}$ given by (4).

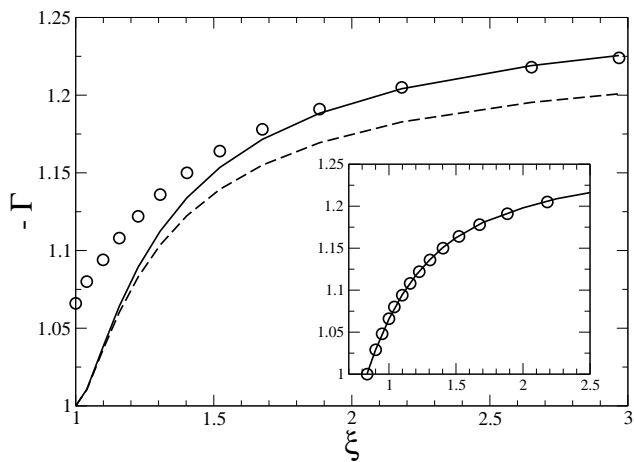


FIG. 3: Preferential interaction coefficient for a 1:1 salt (hence $\mathcal{C} \simeq -1.502$) and $\kappa a = 10^{-2}$. The circles show the numerical solution of PB theory (1), the continuous curve is for (5) with (4) and the dashed line is the prediction of Ref. [9]. Although approximation (4) breaks down at low ξ , the inset shows that $\tilde{\mu}$ following from the solution of Eq. (C2) gives through (5) a Γ (continuous curve), that is in excellent agreement with the “exact one”, shown with circles as in the main graph.

excellent results whenever $\kappa a < 0.1$. To illustrate this, we compare in Figure 5 the potential following from the analytical expression (C1) to its numerical counterpart. We do not display 1:1, 1:2 and 2:1 results since in these cases, Eq. (C1) is obtained from an exact expansion and fully captures the r -dependence of the potential. For the asymmetry 1:3, Fig. 5 shows that the relatively simple form (C1) is very reliable. A similar agreement has been found for all couples $z_-:z_+$ sampled, with the trend that

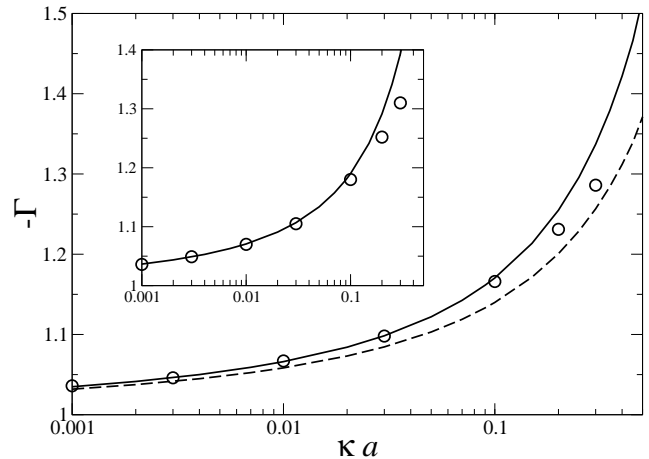


FIG. 4: Same as Fig. 1 for $\xi = 1$ and $z_+/z_- = 1$. The same quantities are shown: our prediction for Γ [Eqs. (5) and (6) with $\mathcal{C} \simeq -1.502$] is compared to that of Ref. [9]. The inset shows $-z_+\Gamma/z_-$ for a 1:2 salt such as MgCl_2 where \mathcal{C} takes the value -1.301. Circles : numerical data; curve : our prediction.

the validity of (C1) extends to larger distances as z_+/z_- is decreased. In this respect, the agreement shown in Fig. 5 for which z_+/z_- is quite high (3), is one of the “worst”

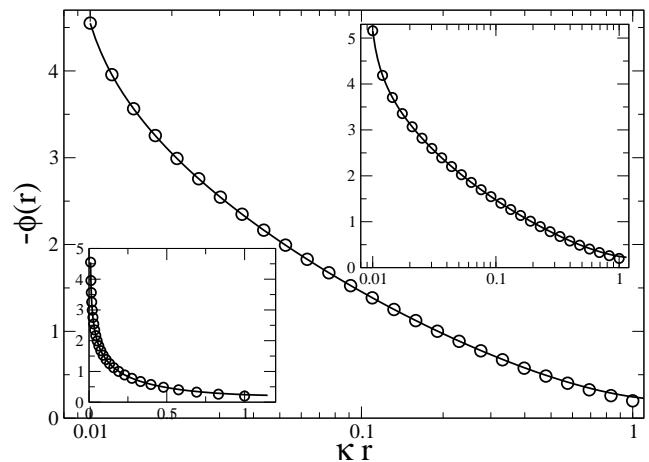


FIG. 5: Opposite of the electric potential versus radial distance in a 1:3 electrolyte with $\kappa a = 10^{-2}$. The continuous curve shows the prediction of Eq. (C1) with $\tilde{\mu}$ given by (4); the circles show the numerical solution of Eq. (1). The potential for $\xi = 2.2$ is shown in the main graph on a log-linear scale, and on a linear scale in the lower inset. The upper inset is for $\xi = 5$.

Conclusion. The poly-ion ion preferential interaction coefficient Γ describes the exclusion of co-ions in the vicinity of a polyelectrolyte in an aqueous solution. We have obtained an accurate expression for Γ in the regime of low salt ($\kappa a < 1$). The present results are particu-

larly relevant for highly charged poly-ions ($z_+\xi > 1$, that is beyond the classical Manning threshold [22]), but are somewhat more general and hold in the range $\xi_c < \xi < 1$, where ξ stands for the line charge per Bjerrum length and ξ_c is a salt dependent threshold, given by Eq. (C5). Our formulae have been shown to hold for arbitrary mixed salts of the form $z_-:z_+$ (magnesium chloride, cobalt hexamine etc). They have been derived from exact expansions valid in 1:1,1:2 and 2:1 cases, from which a more general conjecture has been inferred. The validity of this conjecture, backed up by analytical arguments, has been extensively tested for various values of z_+/z_- , poly-ion charge and salt content. These tests have provided the numerical value of the constant \mathcal{C} reported in Table I, which only depends of the ratio z_+/z_- . As a byproduct of our analysis, we have obtained a very accurate expression for the electric potential in the vicinity of the charged rod ($r < \kappa^{-1}$).

It should be emphasized that the validity of our mean-field description relying on the non-linear Poisson-Boltzmann equation depends on the valency of counter-ions (z_+), and to a lesser extent to the value of z_- [12, 23]. For the 1:1 case in a solvent like water at room temperature, micro-ionic correlations can be neglected up to a salt concentration of 0.1M [8]. For $z_+ \geq 2$ or in solvents of lower dielectric permittivity, they play a more important role. Our results however provide mean-field benchmarks from analytical expressions, from which the effects of correlations may be assessed in cases where they cannot be ignored (see e.g. [8] for a detailed discussion).

Acknowledgments

This work was supported by a ECOS Nord/COLCIENCIAS action of French and Colombian cooperation. G. T. acknowledge partial financial support from Comité de Investigaciones, Facultad de Ciencias, Universidad de los Andes. This work has been supported in part by the NSF PFC-sponsored Center for Theoretical Biological Physics (Grants No. PHY-0216576 and PHY-0225630).

APPENDIX A

In order to explicitly relate the preferential coefficient Γ in (2) to the electric potential, we follow a procedure similar to that which leads to an analytical solution in the cell model, without added salt [24]. Implicit use will be made of the boundary conditions associated to (1). First, integrating Eq. (1), one gets

$$[r'\phi'(r')]_a^r = \frac{\kappa^2}{z_+ + z_-} \int_a^r (e^{-z_+\phi} - e^{z_-\phi}) r' dr', \quad (\text{A1})$$

where the notation $[F(r')]_a^r = F(r) - F(a)$ has been introduced. Then, multiplying Eq. (1) by $r^2\phi'$ and inte-

grating, we obtain

$$\begin{aligned} \frac{z_+ + z_-}{2\kappa^2} [(r'\phi')^2]_a^r &= - \left[r'^2 \frac{e^{-z_+\phi}}{z_+} + r'^2 \frac{e^{z_-\phi}}{z_-} \right]_a^r \\ &+ \int_a^r 2r' \left(\frac{e^{-z_+\phi}}{z_+} + \frac{e^{z_-\phi}}{z_-} \right) dr'. \quad (\text{A2}) \end{aligned}$$

Combining both relations with adequate weights, in order to suppress the integral over counter-ion (+) density, we have

$$\begin{aligned} \int_a^\infty r' (e^{z_-\phi} - 1) dr' &= \frac{z_+ z_-}{\kappa^2} \left(\xi^2 - \frac{2\xi}{z_+} \right) \\ - \frac{a^2}{2(z_+ + z_-)} \{ z_+ (e^{z_-\phi_0} - 1) &+ z_- (e^{-z_+\phi_0} - 1) \} \quad (\text{A3}) \end{aligned}$$

where $\phi_0 = \phi(a)$ is the surface potential. Equation (A3) will turn useful in the formulation of a general conjecture concerning the surface potential ϕ_0 , see Appendix B. We also note that for the systems under investigation here, the surface potential is quite high, and a very good approximation to (A3) is

$$\int_a^\infty r' (e^{z_-\phi} - 1) dr' \simeq \frac{z_+ z_-}{\kappa^2} \left(\xi^2 - \frac{2\xi}{z_+} \right) - \frac{a^2 z_- e^{-z_+\phi_0}}{2(z_+ + z_-)} \quad (\text{A4})$$

APPENDIX B

We start by analyzing a 1:1 electrolyte, for which it has been shown [19, 20] that the short distance behaviour reads

$$e^{\phi/2} = \frac{\kappa r}{4\mu} \sin \left[2\mu \log \left(\frac{\kappa r}{8} \right) - 2\Psi(\mu) \right] + \mathcal{O}(\kappa r)^4 \quad (\text{B1})$$

where Ψ denotes the argument of the Euler Gamma function $\Psi(x) = \arg[\Gamma(ix)]$ [19, 20]. In (B1), μ denotes the smallest positive root of

$$\tan [2\mu \log(\kappa a/8) - 2\Psi(\mu)] = \frac{2\mu}{\xi - 1}. \quad (\text{B2})$$

Expressions (B1) and (B2) require that ξ exceeds a salt dependent threshold [denoted ξ_c below and given by Eq. (C5)] that is always smaller than 1 [18]. They thus always hold for $\xi \geq 1$ and in particular encompass the interesting limiting case $\xi = 1$, which is sufficient for our purposes. For large ξ , we have proposed in [18] an approximation which amounts to linearizing the argument of the tangent in (B1) in the vicinity of $-\pi$, and similarly linearizing Ψ to first order: $\Psi(x) \simeq -\pi/2 - \gamma x + \mathcal{O}(x^3)$ where γ is the Euler constant, close to 0.577. It turns out however that finding accurate expressions for $\exp(-z_+\phi_0)$, which is useful for the computation of the preferential interaction coefficient, requires to include the first non-linear correction in the expansion of the tangent. After some

algebra, we find :

$$\mu \simeq \frac{-\pi/2}{\log(\kappa a) + \mathcal{C} - (\xi - 1)^{-1}} + \frac{\pi^3}{6(\log(\kappa a) + \mathcal{C} - (\xi - 1)^{-1})^4} \times \left[\frac{1}{(\xi - 1)^3} + \frac{\psi^{(2)}(1)}{8} \right] \quad (\text{B3})$$

where the constant $\mathcal{C} = \mathcal{C}^{1:1}$ reads $\mathcal{C}^{1:1} = \gamma - \log 8 \simeq -1.502$ and $\psi^{(2)}(1) = d^3 \ln \Gamma(x)/dx^3|_{x=1}$. From (B3) and (B1) where the sinus is expanded to third order, we obtain

$$(\kappa a)^2 e^{-\phi_0} \simeq 4[(\xi - 1)^2 + \tilde{\mu}^2] \quad (\text{B4})$$

where $\tilde{\mu}$ is given by

$$\tilde{\mu} \simeq \frac{-\pi}{\log(\kappa a) + \mathcal{C} - (z_+ \xi - 1)^{-1}}. \quad (\text{B5})$$

In writing (B5), we have introduced the change of variable $\tilde{\mu} = 2\mu$ [25]. The reason is that similar changes for other electrolyte asymmetries allows to put the final result in a ‘‘universal’’ (electrolyte independent) form, see below. A similar reason holds for introducing z_+ , here equal to 1, in the denominator of (B5).

The functional proximity between our expressions and those reported in [9] in the very same context is striking. We note however that our $\tilde{\mu}$ (denoted β in [9]) involves a different constant \mathcal{C} . More importantly, the functional form of (B1) differs from that given in [9]. The comparison of the performances of our results with those of [9] is addressed below, and is also discussed in the main text.

Performing a similar analysis as above in the 1:2 case where $z_+ = 2$ and $z_- = 1$, we obtain from the expressions derived in [18]:

$$(\kappa a)^2 e^{-z_+ \phi_0} \simeq 3[(\xi - 1)^2 + \tilde{\mu}^2] \quad (\text{B6})$$

and similarly, in the 2:1 case ($z_+ = 1$, $z_- = 2$):

$$(\kappa a)^2 e^{-z_+ \phi_0} \simeq 6[(\xi - 1)^2 + \tilde{\mu}^2]. \quad (\text{B7})$$

In both cases, provided again that ξ is not too low (see below) $\tilde{\mu}$ is given by (B5) [26], with however a different numerical value for \mathcal{C} [$\mathcal{C}^{1:2} = \gamma - (3 \log 3)/2 - (\log 2)/3 \simeq -1.301$ and $\mathcal{C}^{2:1} = \gamma - (3 \log 3)/2 - \log 2 \simeq -1.763$].

The similarity of expressions (B4), (B6) and (B7) leads to conjecture that this form holds for any $z_-:z_+$ electrolyte :

$$(\kappa a)^2 e^{-z_+ \phi_0} \simeq \mathcal{A}[(z_+ \xi - 1)^2 + \tilde{\mu}^2]. \quad (\text{B8})$$

We then have to determine the prefactor \mathcal{A} as a function of z_+ and z_- . To this end, we make use of the exact relation (A3) [or equivalently (A4)], where in the limit of large ξ , the lhs is finite while the two terms on the rhs

diverge. This yields the leading order behaviour :

$$(\kappa a)^2 \exp(-z_+ \phi_0) \stackrel{\xi \rightarrow \infty}{\sim} 2 \frac{z_+ + z_-}{z_+} (z_+ \xi - 1)^2. \quad (\text{B9})$$

It then follows that $\mathcal{A} = 2(z_+ + z_-)/z_+$ so that our general expression (B8) takes the form:

$$(\kappa a)^2 e^{-z_+ \phi_0} \simeq 2 \frac{z_+ + z_-}{z_+} [(z_+ \xi - 1)^2 + \tilde{\mu}^2]. \quad (\text{B10})$$

This expression holds regardless of the approximation used for $\tilde{\mu}$. If Eq. (B5) is used, then $z_+ \xi$ should not be too close to unity (see appendix C for more general results including the case $z_+ \xi = 1$).

In order to test the accuracy of (B10) in conjunction with (B5), we have solved numerically Eq. (1) for several values of $\kappa a < 1$ and electrolyte asymmetry and checked that for several different values of $z_+ \xi > 1$, the quantity

$$\mathcal{Q} = -\pi \left[(\kappa a)^2 e^{-z_+ \phi_0} \frac{z_+}{2(z_+ + z_-)} - (z_+ \xi - 1)^2 \right]^{-1/2} - \log(\kappa a) + (z_+ \xi - 1)^{-1} \quad (\text{B11})$$

is a constant \mathcal{C} , which only depends on z_+/z_- but not on salt and ξ [it should be borne in mind that Eq. (B5) is a small κa and large ξ expansion, which becomes increasingly incorrect as κa is increased and/or ξ lowered]. This is quite a stringent test (since the two terms on the rhs of (B11) are large and close) which requires high numerical accuracy. This is achieved following the procedure outlined in [27]. In doing so, we confirm the validity of (B10) and collect the values of \mathcal{C} given in Table I. In the 1:1 case, we predict that $\mathcal{C} = \gamma - \log 8 \simeq -1.507$, in excellent agreement with the numerical data of Figure 6. On the other hand, the prediction of Ref. [9] that \mathcal{Q} reaches a constant close to -1.90 (shown by the horizontal dashed line in Fig 6) is incorrect. Figure 6 shows that the quality of expression (B10) deteriorates when κa increases, as expected. It is noteworthy however that for $\kappa a = 10^{-1}$, its accuracy is excellent whenever $\xi > 2$. The inset of Fig. 6 shows the validity of (B10) for a 3:1 electrolyte. When $z_+ \xi$ is close to 1, Eq. (B5) becomes an irrelevant approximation to the solution of (B2), and can therefore not be inserted into the general formula (B10). This explains the large deviations between \mathcal{Q} and the asymptotic value \mathcal{C} observed in Fig. 6 for the lower values of ξ reported. We come back to this point in Appendix C.

The present results hold for $z_+ \xi > 1 + \mathcal{O}(1/|\log \kappa a|)$. In this regime, our analysis shows that Eq. (B10) [with $\tilde{\mu}$ given by (B5)] is correct up to order $1/\log^4(\kappa a)$ for any (z_-, z_+) . On the other hand the results of [9], valid in the 1:1 case, appear to be correct to order $1/\log^2(\kappa a)$. In addition, our expression for the surface potential may be generalized to a broader range of ξ values and an expression for the short distance dependence of the electric potential may also be provided. This is the purpose of appendix C.

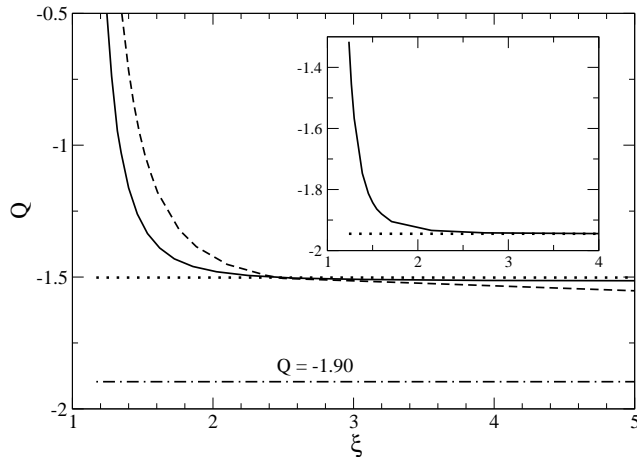


FIG. 6: Plot of the quantity Q defined in (B11) versus line charge ξ for a 1:1 electrolyte at $\kappa a = 10^{-3}$ (continuous curve) and $\kappa a = 10^{-1}$ (dashed curve). The value reached at large ξ is compared to the prediction of [9] $Q \rightarrow e^\gamma + \log 2 - \gamma \simeq -1.90$ (horizontal dashed-dotted line) whereas Eqs. (B10) and (B5) imply $Q \rightarrow \gamma - \log 8 \simeq -1.50$, shown by the horizontal dotted line. The inset shows the same quantity for a 3:1 electrolyte at $\kappa a = 10^{-5}$ [such a very low value is required to determine precisely the value of the asymptotic constant \mathcal{C} , that can subsequently be used at experimentally relevant (higher) salt concentrations]. Here, we obtain $Q \rightarrow -1.94$ (dotted line) which is the value reported for \mathcal{C} in Table I.

APPENDIX C

In Appendix B, the “universal” results valid for all (z_+, z_-) have been unveiled partly by a change of variable $\mu \rightarrow \tilde{\mu}$ from existing expressions [18]. In light of these results, and of their accuracy (assessed in particular by the precision reached for the preferential interaction coefficient), it is tempting to go further without invoking approximations of (B2), or related expressions for other asymmetries than 1:1. Inspection of the results given in [18] for the 1:1, 1:2 and 2:1 cases lead, with again the help of (A4), to the conjecture that

$$e^{z_+\phi/2} \simeq \frac{-\kappa r}{\tilde{\mu}} \sqrt{\frac{z_+}{2(z_+ + z_-)}} \sin[\tilde{\mu} \log(\kappa r) + \tilde{\mu} \mathcal{C}] \quad (\text{C1})$$

with

$$\tan[\tilde{\mu} \log(\kappa a) + \tilde{\mu} \mathcal{C}] = \frac{\tilde{\mu}}{z_+\xi - 1}. \quad (\text{C2})$$

We emphasize that (C1), much as (B1), is a short distance expansion and typically holds for $\kappa r < 1$ (hence the requirement that $\kappa a < 1$). In appendix D we give further analytical support for conjecture (C1). A typical plot showing the accuracy of (C1) is provided in the main text (Fig. 5). For $\kappa r < 0.1$, the agreement with the exact result is better than 0.1%, and becomes progressively worse at higher distances (20% disagreement at $\kappa r = 1$).

From (C1), it follows that the integrated charge $q(r)$ in a cylinder of radius r [that is $q(r) = -r\phi'(r)/2$] reads

$$z_+q(r) = -1 + \tilde{\mu} \tan \left[\tilde{\mu} \log \left(\frac{r}{R_M} \right) \right] \quad (\text{C3})$$

where the so-called Manning radius [18, 28, 29] is given by

$$\kappa R_M = \exp \left(-\mathcal{C} - \frac{\pi}{2\tilde{\mu}} \right). \quad (\text{C4})$$

The Manning radius is a convenient measure of the counterion condensate thickness. It is the point r where not only $z_+q(r) = 1$ but also where $q(r)$ versus $\log r$ exhibits an inflection point [30]. For high enough ξ , the logarithmic dependence of $1/\tilde{\mu}$ with salt [see (B5)] is such that $R_M \propto \kappa^{-1/2}$.

The two relations (C1) and (C2) encompass those given in Appendix B and allow to investigate the regime $z_+\xi_c < z_+\xi$, and in particular the case $z_+\xi = 1$, the so-called Manning threshold [5]. However, (C1) and (C2) are not valid for $\xi < \xi_c$, with

$$z_+\xi_c = 1 + \frac{1}{\log \kappa a + \mathcal{C}}. \quad (\text{C5})$$

Note that $\xi_c < 1$, since the constant \mathcal{C} is negative and that salt should fulfill $\kappa a < 1$. For $\kappa a = 10^{-2}$ and $z_+/z_- = 1$, we obtain $\xi_c \simeq 0.836$. This is precisely the point where $-\Gamma = 1$ in the inset of Fig. 3. This inset also shows that the value of Γ resulting from the use of the solution of (C2) is remarkably accurate.

At this point, it seems useful to investigate the Manning threshold case $z_+\xi = 1$ (which corresponds to the onset of counterion condensation when $\kappa a \rightarrow 0$ [5, 18, 30]). It is readily seen that the solution of (C2) reads

$$\tilde{\mu} \stackrel{z_+\xi=1}{=} \frac{-\pi/2}{\log(\kappa a) + \mathcal{C}}, \quad (\text{C6})$$

which should be inserted in (C1) to obtain the potential profile, or in (5) to get the interaction coefficient.

APPENDIX D

In this appendix we give further support for the conjecture (C1) which gives the short-distance expansion of the electric potential. Let us suppose initially that the charge is below the Manning threshold $\xi < \xi_c$. It is straightforward to verify that Poisson–Boltzmann equation (1) admits solutions which behave as $\phi(r) = -2A \ln(\kappa r) + \ln B + o(1)$ for $\kappa r \ll 1$. Injecting this expansion into equation (1) allows us to compute higher order terms. To study the regime beyond the Manning threshold, we compute all higher order terms of the form $r^{2n(1+z_+A)}$ (for a negatively charged macroion) and

$r^{2n(1-z_-A)}$ (for a positively charged macroion), with n a positive integer. These terms turn out to present themselves as the series expansion of the logarithm, thus re-summing them we obtain

$$\begin{aligned} \phi(r) = & -2A \ln(\kappa r) + \ln B \\ & + \frac{2}{z_+} \ln \left[1 - \frac{z_+ B^{-z_+} (\kappa r)^{2(1+z_+A)}}{8(z_+ + z_-)(1 + z_+A)^2} \right] \\ & - \frac{2}{z_-} \ln \left[1 - \frac{z_- B^{z_-} (\kappa r)^{2(1-z_-A)}}{8(z_+ + z_-)(1 - z_-A)^2} \right] + \dots \end{aligned} \quad (\text{D1})$$

The dots represent terms of order $r^{2n(1+z_+A)+2m(1-z_-A)}$ with n and m two nonzero positive integers. When the Manning threshold is approached, $z_+A + 1 = 0$ for negatively charged macroion, the terms $r^{2n(1+z_+A)}$ (second line of Eq. (D1)) become of order one, but the rest of the terms (third line of Eq. (D1) and dots) remain higher order: a change in the small distance behavior of ϕ occurs. A similar situation is reached for $1 - z_-A = 0$ which is the Manning threshold for a positively charged macroion.

A and B in the previous equations are constants of integration, which should be determined with the boundary conditions $r\phi'(r) = 2\xi$ at the polyion radius ($r = a$) and $\phi \rightarrow 0$ for $r \rightarrow \infty$. Thus to proceed further, we have to connect the long and the short distance behavior of ϕ . This connection problem has been only solved in the cases 1:1, 1:2 and 2:1 in Refs. [19, 31]. In particular, once A has been chosen (notice that for $a = 0$, $A = -\xi$), B should be one and only one function of A in order to satisfy $\phi \rightarrow 0$ for $r \rightarrow \infty$. The results from [19, 31] show that

$$\begin{aligned} B &= 2^{6A} \gamma((1+A)/2)^2 \quad (1:1) \\ B &= 3^{3A} 2^{2A} \gamma(2(1+A)/3) \gamma((1+A)/3) \quad (1:2) \\ B &= 3^{3A} 2^{2A} \gamma((1+2A)/3) \gamma((2+A)/3) \quad (2:1) \end{aligned} \quad (\text{D2})$$

where $\gamma(x) = \Gamma(x)/\Gamma(1-x)$. B turns out to have some interesting properties in the cases 1:1, 1:2 and 2:1, where

its exact expression (D2) is known. Namely, at the Manning threshold $1 + z_+A = 0$,

$$\lim_{A \rightarrow -1/z_+} \frac{z_+ B^{-z_+}}{8(z_+ + z_-)(1 + z_+A)^2} = 1 \quad (\text{D3})$$

Furthermore if we put $1 + z_+A = i\tilde{\mu}$, and define

$$e^{2i\Psi(\tilde{\mu})} = \frac{z_+ B^{-z_+}}{8(z_+ + z_-)(1 + z_+A)^2} \quad (\text{D4})$$

then for $\tilde{\mu} \in \mathbb{R}$, $\Psi(\tilde{\mu}) \in \mathbb{R}$ is a *real* function of $\tilde{\mu}$, with $\Psi(0) = 0$.

Let us now study the regime beyond the Manning threshold for a negatively charged macroion. From Eq. (D1) we can write

$$e^{z_+\phi(r)/2} \sim (\kappa r)^{-z_+A} B^{z_+/2} \left(1 - \frac{z_+ B^{-z_+} (\kappa r)^{2(1+z_+A)}}{8(z_+ + z_-)(1 + z_+A)^2} \right) \quad (\text{D5})$$

neglecting terms of higher order when z_+A is close to -1 .

Let us conjecture that the properties of B as a function of A presented above hold in the general case $z_- : z_+$. Then using the parameter $\tilde{\mu}$ defined above we find after some simple algebra

$$\begin{aligned} e^{z_+\phi(r)/2} = & \frac{-\kappa r}{\tilde{\mu}} \sqrt{\frac{z_+}{2(z_+ + z_-)}} \sin[\tilde{\mu} \log(\kappa r) + \Psi(\tilde{\mu})] \\ & + O(r^{3+2z_-/z_+}) \end{aligned} \quad (\text{D6})$$

Recalling that $|\tilde{\mu}| \ll 1$ we can approximate $\Psi(\tilde{\mu}) \simeq \tilde{\mu}\mathcal{C}$, where $\mathcal{C} = \Psi'(0)$. Replacing this approximation into (D6) and imposing the boundary condition $a\phi'(a) = 2\xi$ leads to (C1) and (C2). Numerical values obtained for the constants \mathcal{C} are reported in Table I, for different charge asymmetries $z_- : z_+$. The previous analysis shows that analytical predictions for \mathcal{C} could be made if the connection problem is solved and the equivalent of expressions (D2) are found for the general case $z_- : z_+$.

-
- [1] C.F. Anderson and M.T. Record Jr, *Annu. Rev. Phys. Chem.* **33**, 191 (1984).
[2] H. Eisenberg, *Biological Macromolecules and Polyelectrolytes in Solution*, Clarendon, Oxford (1976).
[3] J.A. Schellman, *Biophys. Chem.* **37**, 121 (1990).
[4] S.M. Timasheff, *Biochemistry* **31**, 9857 (1992).
[5] G.S. Manning, *J. Chem. Phys.* **51**, 924 (1969).
[6] F. Oosawa, *Polyelectrolytes*, Dekker, New York (1971).
[7] K.A. Sharp, *Biopolymers* **36**, 227 (1995).
[8] H. Ni, C.F. Anderson and M.T. Record Jr, *J. Phys. Chem. B* **103**, 3489 (1999).
[9] I.A. Shkel, O.V. Tsodikov and M.T. Record Jr, *Proc. Natl. Acad. Sci. USA* **99**, 2597 (2002).
[10] C.H. Taubes, U. Mohanty and S. Chu, *J. Phys. Chem. B* **109**, 21267 (2005).
[11] M. Gueron, J.-Ph. Demaret and M. Filoche, *Biophys. Journal* **78**, 1070 (2000).
[12] Y. Levin, *Rep. Prog. Phys.* **65**, 1577 (2002).
[13] In the 1:1 case, our definition differs from the more standard one as found e.g. in [9] by a factor 4ξ . The reason for doing so is that this allows easier comparison of the salt dependence of Γ for different values of the poly-ion charge.
[14] F.G. Donnan, *Chem. Rev.* **1**, 73 (1924).
[15] I.A. Shkel, O.V. Tsodikov and M.T. Record Jr, *J. Phys. Chem. B* **104**, 5161 (2000).
[16] M. Aubouy, E. Trizac, L. Bocquet, *J. Phys. A: Math. Gen.* **36**, 5835 (2003).
[17] G. Téllez and E. Trizac, *Phys. Rev. E* **70**, 011404 (2004).
[18] E. Trizac and G. Téllez, *Phys. Rev. Lett* **96**, 038302 (2006); G. Téllez and E. Trizac, *J. Stat. Mech.* P06018 (2006).
[19] B.M. McCoy, C.A. Tracy and T.T. Wu, *J. Math. Phys.* **18**, 1058 (1977).

- [20] J.S. McCaskill and E.D. Fackerell, J. Chem. Soc., Faraday Trans. 2 **84**, 161 (1988).
- [21] C.A. Tracy and H. Widom, Physica A **244**, 402 (1997).
- [22] We emphasize that accurate results for Γ , ϕ etc may be obtained for $\xi < \xi_c$ from the results given in [18]. We did not investigate this regime here, since it is of little relevance for nucleic acids.
- [23] A.Y. Grosberg, T.T. Nguyen and B.I. Shklovskii, Rev. Mod. Phys. **74**, 329 (2002).
- [24] R.M. Fuoss, A. Katchalsky and S.F. Lifson, P. Natl. Acad. Sci. USA **37**, 579 (1951).
- [25] It then appears that the expression given for $\tilde{\mu} = 2\mu$ in (B5) corresponds to the dominant term only in (B3) (the first one on the rhs).
- [26] Compared to the expressions given in [18] where a parameter μ plays a key role, the corresponding change of variables should be performed: $\tilde{\mu} = 3\mu$ (1:2 case) and $\tilde{\mu} = 3\mu/2$ for 2:1 electrolytes.
- [27] E. Trizac, L. Bocquet, M. Aubouy and H.H. von Grünberg, Langmuir **19**, 4027 (2003).
- [28] M. Gueron and G. Weisbuch, Biopolymers **19**, 353 (1980).
- [29] B. O'Shaughnessy and Q. Yang, Phys. Rev. Lett. **94**, 048302 (2005).
- [30] M. Deserno, C. Holm and S. May, Macromolecules **33**, 199 (2000).
- [31] C.A. Tracy and H. Widom, Commun. Math. Phys. **190**, 697 (1998).